Eur. Phys. J. B **30**, 571–575 (2002)
DOI: 10.1140/epjb/e2002-00415-3

THE EUROPEAN PHYSICAL JOURNAL B

Spatial orders appearing at instabilities of synchronous chaos of spatiotemporal systems

Shihong Wang[1], Jinghua Xiao[3,1], Xingang Wang[2], Bambi Hu[3], and Gang Hu[4,2,5,a]

[1] Science school, Beijing University of Posts and Telecommunications, Beijing 100876, PR China
[2] Department of Physics, University of Normal Beijing, Beijing 100875, PR China
[3] Centre of Nonlinear Studies and Department of Physics, Hong Kong Baptist University, Hong Kong, PR China
[4] China Center for Advanced Science and Technology (CCAST) (World Laboratory), PO Box 8730, Beijing 100080, PR China
[5] Institute of Low Energy Physics, Beijing Normal University, Beijing 100875, PR China

Received 31 July 2002 / Received in final form 20 November 2002
Published online 31 December 2002 –

Abstract. Various spatial orders introduced by the instabilities of synchronous chaotic state of spatiotemporal systems are investigated by considering coupled map lattice and chaotic partial differential equation. In particular, the motions of on-off intermittent states at the onset of the instabilities are studied in detail. The chaotic desynchronized patterns can be described by a simple universal form, including three parts: the synchronous chaos; a spatially ordered pattern, determined by the unstable mode of the reference synchronous chaos; and on-off intermittency of the scale of this given pattern.

PACS. 05.45.-a Nonlinear dynamics and nonlinear dynamical systems – 05.45.Jn High-dimensional chaos – 05.45.Xt Synchronization; coupled oscillators

Chaos synchronization has attracted great attention after the pioneering work of Pecora and Carroll [1–6]. In this field one of the most important topics is the synchronization of coupled spatiotemporal systems. Many papers considering this problem have focused on the condition of instability of synchronous chaos [7–9]. It has been made clear that some interesting partially synchronous patterns can appear when desynchronization of synchronous chaos occurs [10,11], and on-off intermittency can be observed between desynchronous chaotic oscillators (or, desynchronous clusters of oscillators) [2,9–11]. However, a very important aspect, *i.e.*, the spatial ordering after the desynchronization of chaos, has not yet been studied apart from the brief discussion of [4], and this problem is of crucial significance for the pattern formations from chaotic spatiotemporal systems.

Suppose a stationary or periodic spatiotemporal system is prepared around a certain instability condition, we can then predict the spatiotemporal ordering after the instability by classifying the type of the unstable mode. Now we ask: can we observe any spatial ordering when a synchronous chaos becomes to be desynchronized after certain instability, and can we predict this ordering according to the mode of instability if the answer to the first question is positive? These problems remain unresolved after more than a decade of the study of chaos synchronization, and they are nontrivial since there is a strong intuitive impression that a desynchronous chaos (a basic chaotic motion plus random on-off intermittent bursts between various desynchronous oscillators) looks rather "random" in both time and space.

In this paper, we find that various spatial orders can be clearly seen in desynchronized chaotic states at the onset of different instabilities, and these spatial orders can be well predicted from the linear unstable modes of the reference synchronous chaotic state. We use systems of two-dimensional (2D) coupled map lattice (CML) and 1D chaotic partial differential equation(PDE) as our models to demonstrate the above results, and the validity of the same analysis to coupled chaotic oscillators is also confirmed.

Let us start from a 2D CML model,

$$x_{n+1}(j_1,j_2) = (1-\varepsilon)f(x_n(j_1,j_2)) + \frac{\varepsilon}{4}(f(x_n(j_1+1,j_2)) + f(x_n(j_1-1,j_2)) + f(x_n(j_1,j_2+1)) + f(x_n(j_1,j_2-1))) \quad (1)$$

where we use periodic boundary condition of system size N for both j_1 and j_2. The function $f(x)$ is the logistic map $f(x) = ax(1-x)$. We first fix $a = 3.7$, at which the motion of single map is chaotic, and $N = 5$ for simulations.

In Figure 1a we plot the largest three Lyapunov exponents LEs of the CML vs the coupling ε by numerically computing equation (1). It is clear that stable synchronous chaos with a single positive LE $\lambda_1 \approx 0.354$ exists in the interval $0.864 \approx \varepsilon_1 < \varepsilon < \varepsilon_2 \approx 0.941$, and bifurcations to desynchronous chaos occur as the coupling

[a] e-mail: hugang@sun.ihep.ac.cn

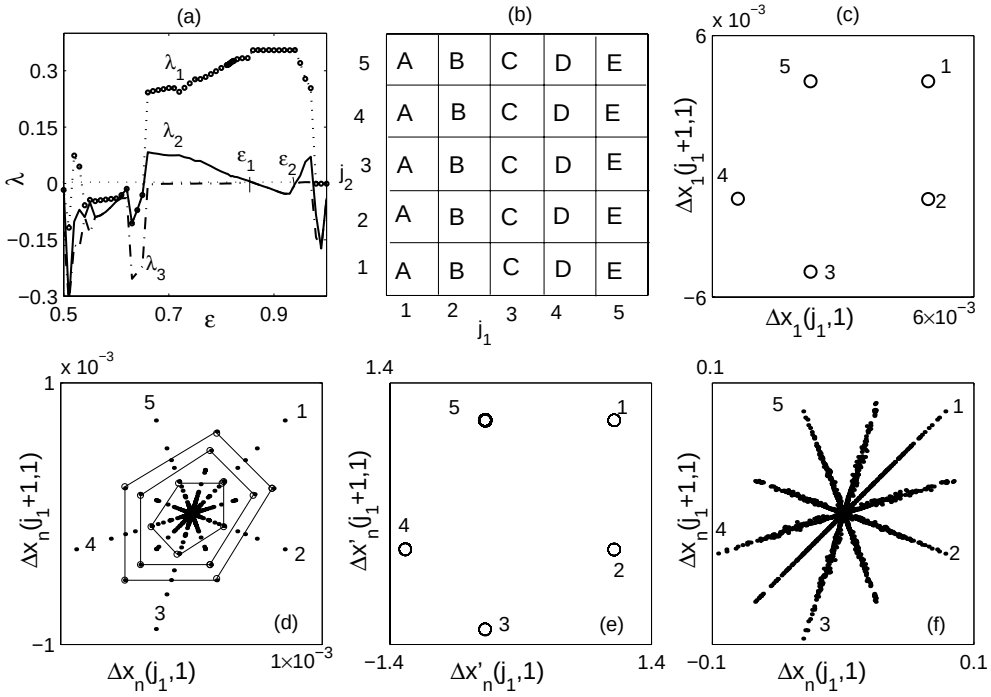

Fig. 1. $a = 3.7$ and $N = 5$. The synchronous chaos is stable in the region $0.864 \approx \varepsilon_1 < \varepsilon < \varepsilon_1 \approx 0.941$. (a) The three largest LEs numerically computed from equation (1). The synchronous chaos becomes unstable when the second largest LE crosses zero to positive. A long wave mode $(1, 0)$ instability and a short wave mode $(2, 2)$ instability of the synchronous chaos occur at ε_1 and ε_2, respectively. (b)–(f) $\varepsilon = 0.833$. (b) The schematic pattern of the desynchronous chaotic state. Each letter indicates a cluster of sites having identical chaotic trajectory for all time after the transient. Different letters show desynchronized clusters. (c) The spatial map at an arbitrary iteration n. $\Delta x_n(j_1, j_2) = x_n(j_1, j_2) - \overline{x}_n$, $\overline{x}_n = \frac{1}{5}\sum_{j_1=1}^{5} x_n(j_1, j_2)$. (d) The same as (c) with many maps for different iterations plotted together. For showing pattern dynamics of the system we arbitrarily choose three successive iterations and link the dots of each iteration to form a frame. The three frames show satisfactory similarity (may with opposite orientations due to the opposite signs of scaling factor). (e) The same as (d) with all variables rescaled by $\Delta x'_n(j_1, j_2) = \Delta x_n(j_1, j_2)/\Delta x_n(1, 1)$. (f) The same as (d) by considering iterations having much larger $\Delta x_n(j_1, j_2)$.

crosses either the small (ε_1) or the large (ε_2) critical values when the second largest LE (*i.e.*, the largest transverse LE) crosses zero. The types of bifurcations at ε_1 and ε_2 can be analytically predicted by linearizing equation (1) around the reference synchronous chaos. It can be easily shown that a long wave (the mode $k_\mu = 1$, $k_\nu = 0$ or $k_\mu = 0, k_\nu = 1$) instability occurs by decreasing ε to cross the ε_1 boundary; and a short wave (the mode $k_\mu = 2$, $k_\nu = 2$) instability appears by increasing ε over the ε_2 threshold, where the linear modes k_μ and k_ν are defined as $\eta_n(k_\mu, k_\nu) = \sum_{j_1}\sum_{j_2} \mathrm{e}^{\mathrm{i}k_\mu j_1 + \mathrm{i}k_\nu j_2}[x_n(j_1, j_2) - x_n]$, with x_n being the trajectory of the synchronous chaos.

Let us first consider the case of the long wave instability. We take $\varepsilon = 0.833$ and numerically compute equation (1). The system motion is chaotic, and on-off intermittency can be clearly observed between the desynchronized sites. Now we go further to study the characteristic features and spatial order of this on-off intermittent chaotic motion. In Figure 1b we show schematically the spatial pattern of the system, where different letters show different clusters of sites having desynchronous motions, and sites indicated by a same letter have exactly same chaotic trajectory for all time after the transient. An interesting feature of this pattern is that all sites in a same vertical line (with the same j_1 index) are synchronized to each other, and this structure confirms the long wave instability of mode $k_\nu = 0$. In order to investigate the possible spatial order among the desynchronized clusters in Figure 1b, we plot a spatial map of $\Delta x_n(j_1, j_2)$ *vs.* $\Delta x_n(j_1 + 1, j_2)$ in Figure 1c for an arbitrarily chosen iteration n, where $\Delta x_n(j_1, j_2) = x_n(j_1, j_2) - \overline{x}_n$, with $\overline{x}_n$ being the spatial average $\overline{x}_n = \frac{1}{5}\sum_{j_1=1}^{5} x_n(j_1, j_2)$, and the numbers j_1s in the figure indicate the positions of the $(\Delta x_n(j_1, j_2),\ \Delta x_n(j_1 + 1, j_2))$ points. In Figure 1c, all the points are arranged in a closed loop in the order of their numbers. This arrangement, together with the vertical-line-synchronization structure of Figure 1b, coincides convincingly with the $(1, 0)$ mode instability at ε_1 of Figure 1a. For confirming the generality of the pattern structure of Figure 1c we present Figure 1d where the map points same as Figure 1c for a large number of iterations are plotted together. The map points in Figure 1d show that all the map patterns for different iterations have very good similarity, especially marking three frames for three sucessive iterations. For verifying this similarity, we reorganize the points in Figure 1d by rescaling all the variables as $\Delta x'_n(j_1, j_2) = \Delta x_n(j_1, j_2)/\Delta x_n(1, 1)$, and plot these rescaled map points in Figure 1e. All the

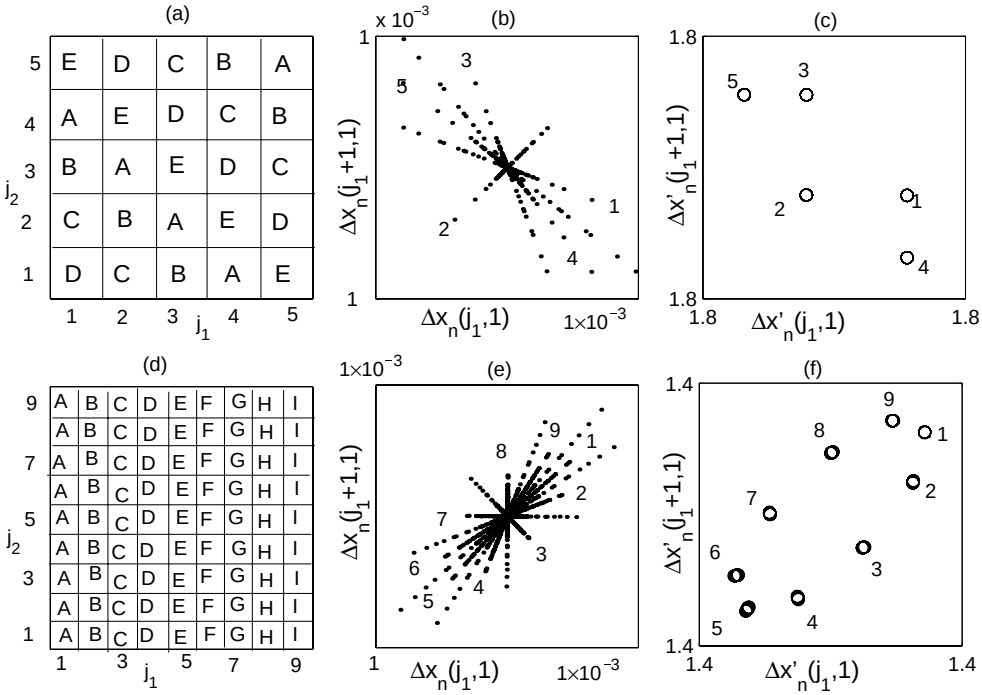

Fig. 2. (a)–(c): The same as Figures 1b, d, and e, respectively, with $\varepsilon = 0.949$, and short wave instability of mode $(2, 2)$ considered. d, e, f: The same as Figures 1b, d, e, respectively, with $a = 3.579$, $N = 9, \varepsilon = 0.795$, and long wave instability of mode $(1, 0)$ considered.

points scattered in each line in Figure 1d concentrate to a single point in (e), in a good approximation, indicating that the spatial patterns for different n resemble each other in shape. Thus, the spatial structure of Figure 1c is well maintained in the manner of similarity during the desynchronized chaotic motion, though the sizes of the corresponding patterns vary considerably and randomly in the on-off intermittency. In Figure 1d the desynchronous variables $\Delta x_n(j_1, j_2)$ are chosen in a time interval where their absolute values are rather small. The desynchronized bursts may become large for some other time periods and for the same parameters, nonlinearity can introduce certain deviation in the pattern similarity. However, all the characteristic features demonstrated above are approximately kept. In Figure 1f, we do the same as Figure 1d by taking the data in a time interval with considerably large $\Delta x_n(j_1, j_2)$. It is clear that the similarity of the desynchronous patterns still exists in Figure 1f, with certain fluctuations.

We can define a quantity $\langle|\Delta x|\rangle = \frac{1}{5T}\sum_{n=1}^{T}\sum_{j_1=1}^{5}|\Delta x_n(j_1, j_2)|$ (where $\sum_{n=1}^{T}$ is over period T which is chosen sufficiently large as 2×10^6) to measure the desynchronization strength. Numerical simulations show that $\langle|\Delta x|\rangle$ has a scaling relation with ε as $\langle|\Delta x|\rangle \propto (\varepsilon_1 - \varepsilon)$, indicating a supercritical bifurcation. And the same kind of bifurcations are also observed for Figures 2 and 3.

The most important conclusion from Figures 1d and e is: the spatiotemporal structure of the desynchronized state at the onset of on-off intermittency can be represented by a universal form

$$x_n(j_1, j_2) = \overline{x}_n + S_n \Delta x'_n(j_1, j_2), \qquad S_n = \Delta x_n(1, 1) \quad (2)$$

where the motion of the entire CML can be described by three quantities. First, $\overline{x}_n$ represents the synchronous chaos, "random" in time and homogeneous (regular) in space; second, the multiple factor S_n indicates the collective behavior of on-off intermittency of the desynchronized elements, which is again random in time. It is significant that in form (2) both the chaotic function $\overline{x}_n$ and the intermittency factor S_n do not include any spatial information, *i.e.*, both functions are scalar and space-independent. All information of the space-dependence is included in the third function $\Delta x'_n(j_1, j_2)$ only, called the normalized desynchronized part, which is well ordered in space. And this space order is determined by the mode of instability of the synchronous chaos. For instance, for our model equation (1), this spatial order is explicitly given (numerically, of course) in Figure 1e, which is dynamically determined by the $(1, 0)$ long wave mode instability, and the scalar factor is nothing by the normalization factor $\Delta x_n(1, 1)$.

Formula (2) is expected to be generally satisfied if the control parameters are taken in a close vicinity of desynchronization bifurcation from synchronous chaos. For instance, it can be directly applied to the short wave instability at ε_2 of Figure 1a. In Figures 2a, b, c, we do

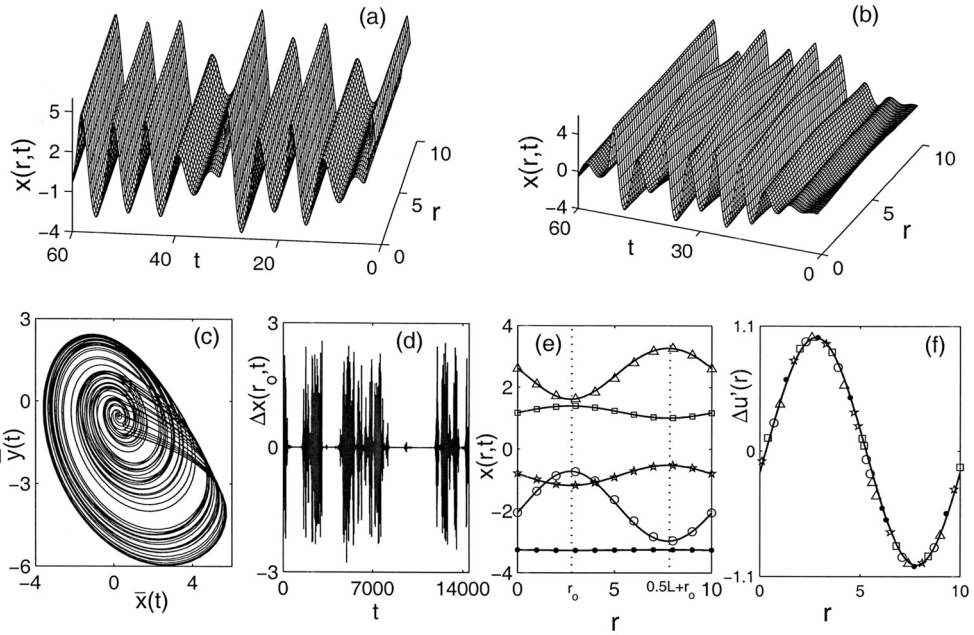

Fig. 3. The numerical results of equations (3). $a = 0.45, b = 2.0, c = 4.0, L = 10$. (a) The spatiotemporal pattern of synchronous chaos of equations (3), which is stable for $D > D_c \approx 0.283$. (b)-(f) $D = 0.275$. (b) A weakly desynchronous chaotic pattern(on-off intermittency) of equations (3). (c) The chaotic trajectory of $\overline{\mathbf{u}}(t)$ in equation (4) in the $(\overline{x}(t), \overline{y}(t))$ plane. $\overline{x}(t) = \frac{1}{L}\int_0^L x(r,t)\mathbf{d}r$, $\overline{y}(t) = \frac{1}{L}\int_0^L y(r,t)\mathbf{d}r$. (d) The scaling function $S_x(t) = \Delta x(r_0, t)$, where $\Delta x(r,t) = x(r,t) - \overline{x}(t)$, and r_0 is such chosen that $|\Delta x(r,t)|$ has maximum for all the time. (e) $x(r,t)$ *vs.* r of equations (3) for five different t's arbitrarily chosen and represented by circles, triangles, squares, disks, and stars, respectively. The space points $r = r_0$ and $r = \frac{L}{2} + r_0$ are the axes of a mirror symmetry, which are kept in the entire on-off intermittency process. All the solid lines are functions $\overline{x}(t) + S_x(t)\cos[\frac{2\pi}{L}(r - r_0)]$ with $S_x(t) = x(r_0, t) - \overline{x}(t)$. (f) The considerably distinctive distribution of (e) are normalized to an identical function by the universal formula equation (4) as $\Delta u'(r) = [x(r,t) - \overline{x}(t)]/\Delta x(r_0, t)$. The solid line is $\cos[\frac{2\pi}{L}(r - r_0)]$, which is typically induced by the $k = 1$ mode instability, and perfectly coincides with the numerical data.

the same as Figures 1b, d and e, respectively, by taking $\varepsilon = 0.949$, slightly larger than ε_2. The partial synchronization of sites in lines parallel to the diagonal in (a) coincides with the $k_\mu = k_\nu$ mode structure. And the fact that the circles 1 to 5 in (c) are arranged in two loops (*i.e.*, in 4π angle) further confirms the $(2, 2)$ short wave mode instability. It is clear that the chaotic and the on-off intermittent motion of Figure 2b can be also described by form (2) in the way precisely the same as that of Figure 1 except that the space-dependent function $\Delta x'_n(j_1, j_2)$ is now explicitly given by Figure 2c for the short wave spatial ordering rather than by Figure 1e for the long wave mode ordering. Moreover, equation (2) is also valid for different system sizes. In Figures 2d, e, and f, we plot the same figures as Figures 1b, d, and e, respectively, by taking $N = 9$ lattice and $a = 3.579$, $\varepsilon = 0.795$, in which the long wave instability occurs at $\varepsilon = \varepsilon_1 \approx 0.810$. It is obvious that all the features appearing in Figure 1 and equation (2) are observed for the system with larger size. Actually, equation (2) is valid for any finite system size $N > 1$. For even larger N we need only to set a to be closer to the accumulation point $a^* = 3.57...$ for obtaining stable synchronous chaos.

The most significant point is that the idea demonstrated in equation (2) is valid for different systems with different spatial dimensions. We have tried both 1D and 2D coupled maps with different system sizes; and examined 1D and 2D coupled chaotic oscillators (*e.g.*, coupled Rossler and Lorenz oscillators); and also investigated 1D chaotic PDEs. In all these cases we find equation (2), the only changes are: we replace the discrete time n in equation (2) by continuous time t for coupled oscillators, and replace both discrete time and space variables in equation (2) by continuous time and space ones for PDEs. In the following we show the results for a 1D extended chaotic Rossler system for manifesting the generality of equation (2).

We take a diffusive 1D Rossler equation with ring structure as our model

$$\dot{x} = -(y + z) + D\partial^2 x/\partial^2 r,$$

$$\dot{y} = x + ay + D\partial^2 y/\partial^2 r,$$

$$\dot{z} = b + (x - c)z + D\partial^2 z/\partial^2 r,$$

$$x(r + L) = x(r), y(r + L) = y(r), z(r + L) = z(r). \quad (3)$$

With $a = 0.45$, $b = 2.0$, and $c = 4.0$, the local dynamics is chaotic. Without losing any generality, we keep $L = 10$. We use the classical explicit difference method for numerical computation and take space step $\Delta r = 0.1$, time step $\Delta t = 0.002 < 0.25(\Delta r)^2$. The correctness of the numerical

results for simulating PDEs is verified by the stability of the output in reducing the space and time steps. For sufficiently large D the system must have stable homogeneous chaos (Fig. 3a). By decreasing D the synchronous chaos loses its stability for certain critical $D = D_c \approx 0.283$ *via* a long wave $k = 1$ mode instability (Fig. 3b). Our main task is to investigate the system dynamics at the onset of the instability $D \leq D_c$.

The desynchronous chaotic pattern shown in Figure 3b can be described by the universal form, a continuous version of equation (2), as

$$\mathbf{u}(r,t) = \overline{\mathbf{u}}(t) + \mathbf{S}(t)\Delta u'(r),$$
$$\Delta u'(r) = \cos\left[\frac{2\pi}{L}(r - r_0)\right] \tag{4}$$

where three quantities together describe the system evolution $\mathbf{u}(r,t) = (x(r,t), y(r,t), z(r,t))$: $\overline{\mathbf{u}}(t) = (\overline{x}(t), \overline{y}(t), \overline{z}(t))$, $\overline{x}(t) = \frac{1}{L}\int_0^L x(r,t)\mathbf{d}r$ (the same for $\overline{y}(t)$ and $\overline{z}(t)$), manifests the synchronous chaotic motion; $\mathbf{S}(t) = (S_x(t), S_y(t), S_z(t)) = (\Delta x(r_0,t), \Delta y(r_0,t), \Delta z(r_0,t))$ shows the scaling factor of the on-off intermittency of the desynchronous part, with $\Delta x(r,t) = x(r,t) - \overline{x}(t)$, and r_0 is such chosen that $\Delta x(r_0,t)$ has maximum $|\Delta x(r,t)|$ for any time; while $\Delta u'(r)$ specifies the spatial order and symmetry of the desynchronous element, which is nothing but the coherent spatial structure induced by the $k = 1$ mode instability of the synchronous chaos. In Figure 3c we plot the trajectory of $\overline{\mathbf{u}}(t)$ in the $(\overline{x}(t), \overline{y}(t))$ plane, which is the orbit of a chaotic Rossler oscillator. In Figure 3d, the scaling factor $S_x(t) = \Delta x(r_0,t)$ is plotted, which shows typical on-off intermittency. And in Figure 3e various spatial distributions of $x(r,t)$ for different t's arbitrarily chosen are plotted while in Figure 3f all the distinctive distributions of (e) are rescaled by $\Delta u'(r) = \Delta x(r,t)/\Delta x(r_0,t)$, which is perfectly coincided with an identical function $\cos[\frac{2\pi}{L}(r - r_0)]$. Again we find that all "randomness" is included in the function $\overline{\mathbf{u}}(t)$ and the scaling factor $\mathbf{S}(t)$, both are, however, space-independent. And all spatial information is included in the normalized function $\Delta u'(r) = \cos[\frac{2\pi}{L}(r - r_0)]$, which is simple, explicit and regular.

In conclusion we have obtained the following. When a synchronous chaos of a spatiotemporal system loses its stability *via* on-off intermittency, coherent and spatially ordered pattern appears for the desynchronous elements. These coherence and order are determined by the unstable mode of the reference state and kept in the random alternations of on and off states in the form of equations (2) and (4). Here we use systems of 2D coupled map lattice and 1D Rossler PDE as our models. The same results are found for coupled chaotic oscillators. And equations (2) and (4) are expected to be universal for the behavior of desynchronization from synchronous chaos of extended different systems with different dimensions and different sizes.

References

1. L.M. Pecora, T.L. Carroll, Phys. Rev. Lett. **64**, 821 (1990)
2. A. Pikovsky, M.G. Rosenblum, G.V. Osipov, J. Kurths, Physica D **104**, 219 (1997)
3. L. Kocarev, U. Parlitz, Phys. Rev. Lett. **76**, 1816 (1996)
4. M. Zhan, G. Hu, J.Z. Yang, Phys. Rev. E **62**, 29632 (2000)
5. M.A. Matias, Phys. Rev. Lett. **78**, 219 (1997)
6. Y.C. Lai, Y. Nagai, C. Grebogi, Phys. Rev. Lett. **79**, 652 (1997)
7. J.F. Heagy, T.L. Carroll, L.M. Pecora, Phys. Rev. Lett. **74**, 4185 (1994)
8. G. Hu, J.Z. Yang *et al.*, Phys. Rev. Lett. **81**, 5314 (1998)
9. L.M. Pecora, Phys. Rev. E **58**, 347 (1998)
10. Belykh *et al.*, Phys. Rev. E **62**, 6332 (2000)
11. Y. Zhang *et al.*, Phys. Rev. E **63**, 026211 (2001)